

# Network Architecture Search for Face Enhancement

Rajeev Yasarla<sup>\*1</sup>, Hamid Reza Vaezi Joze<sup>2</sup>, and Vishal M. Patel<sup>1</sup>

<sup>1</sup>Department of Electrical and Computer Engineering, Johns Hopkins University

<sup>2</sup>Microsoft

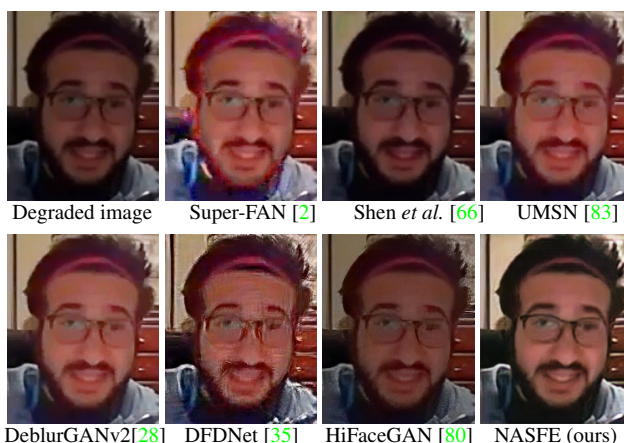
{ryasar11,vpatel36}@jhu.edu, hava@microsoft.com

## Abstract

Various factors such as ambient lighting conditions, noise, motion blur, etc. affect the quality of captured face images. Poor quality face images often reduce the performance of face analysis and recognition systems. Hence, it is important to enhance the quality of face images collected in such conditions. We present a multi-task face restoration network, called Network Architecture Search for Face Enhancement (NASFE), which can enhance poor quality face images containing a single degradation (i.e. noise or blur) or multiple degradations (noise+blur+low-light). During training NASFE uses clean face images of a person present in the degraded image to extract the identity information in terms of features for restoring the image. Furthermore, the network is guided by an identity-loss so that the identity information is maintained in the restored image. Additionally, we propose a network architecture search-based fusion network in NASFE which fuses the task-specific features that are extracted using the task-specific encoders. We introduce FFT-op and deveiling operators in the fusion network to efficiently fuse the task-specific features. Comprehensive experiments on synthetic and real images demonstrate that the proposed method outperforms many recent state-of-the-art face restoration and enhancement methods in terms of quantitative and visual performance.

## 1. Introduction

In the era of COVID-19, the use of video communication tools such as Zoom, Skype, Webex, MS Teams, Google Meet etc. has increased drastically. In many cases, images/videos captured by these video conferencing tools are of poor quality due to low-light ambient conditions, noise, motion artifacts etc. Figure 1 shows an example of such an image taken during a video conference. Hence, it is impor-



DeblurGANv2[28] DFDNet [35] HiFaceGAN [80] NASFE (ours)  
Figure 1: Sample results on the face with multiple degradations like blur, noise and low-light conditions. Restoration methods such as [48, 66, 2, 83, 35, 80] fail to reconstruct a high quality clean face image. In contrast, the proposed NASFE network produces a high quality face image.

tant to enhance the quality of face images collected in such conditions. Furthermore, restoration of degraded face images is an important problem in many applications such as human computer interaction (HCI), biometrics, authentication and surveillance.

Existing face image restoration and enhancement methods are designed to address only a single type of degradation such as blur, noise or low-light. However, in practice face images might have been collected in the presence of multiple degradations (i.e. noise + blur+ low-light). Hence, it is important to enhance the quality of face images collected in such conditions. In this paper, we address the problem of restoring a single face image degraded by multiple degradations (noise+blur+low-light). To the best of our knowledge, we are first ones to address such a multi-task image restoration problem where a single network is able to remove the effects of low-light conditions, noise, and blur

<sup>\*</sup>Work performed during internship at Microsoft

simultaneously.

Face images are structured and informative when compared to natural images. Methods such as [48, 66, 2, 83] extract structured information from faces in the form of semantic maps or exemplar masks in order to super-resolve or remove blur from the degraded face images. This way of extracting facial semantic information is extremely difficult when there are multiple degradations present in the image and as a result may lead to poor restoration performance. Recently, HiFaceGAN [80] addressed face restoration using a multi-stage semantic generation framework. The performance of this method relies heavily on the features extracted from the degraded faces for capturing semantic information. However, it is difficult to learn semantic structure from the noisy features corresponding to multiple degradations. Recently, DFDNet [35] proposed a dictionary-based method to produce a high-resolution face image from a low-resolution input. Note that super resolution is a relatively easy task compared to restoring an image from multiple degradations since semantic information cannot be easily extracted from the images with multiple degradations. As shown in Figure 1 even though state-of-the-art face image restoration methods such as [48, 66, 2, 83, 35, 80] are retrained on multiple degradations, they fail to reconstruct a high-quality clean face image.

Recently, Li *et al.* [36] proposed a blind face restoration method by utilizing multi-exemplar images and adaptive fusion of features from guidance and degraded images. An important point to note here is that computation of the guidance image also relies on extracting the structured information (i.e. landmarks) from degraded face image and clean face image. Since structured information extracted from a degraded image with multiple degradations is not reliable, this way of computing a guidance image will not be helpful in addressing the proposed problem of multi-task face image restoration. To address this problem, we propose a way of using clean face images corresponding to same person in the degraded image to restore the image. These clean images, which may be taken in different scenarios at different times, help us extract the identity information using VG-GFace features [51]. Since these images may have different styles due to contrast or illumination, we apply Adaptive-Instance normalization (AdaIN) [21] on the extracted VG-GFace features to transform the style to that of the degraded face image. We also use these extracted features and propose a novel identity-loss,  $\mathcal{L}_{iden}$ , for training the network.

The proposed multi-task face restoration problem can be considered as an many-to-one feature mapping problem, i.e. extracting task specific features (i.e. noisy, blur, and low-light enhancement features) and fusing them to get features corresponding to the clean image. The fused features can then be used by a decoder to restore the face image. One

can clearly see the importance of fusion in this framework. Rather than naively using Res2Blocks [15] or convolutional blocks in the fusion network, one can learn an architecture for fusion which may lead to better restoration. To this end, we propose a neural architecture search-based approach [40, 41] for learning the fusion network architecture. Additionally, we introduce FFT-op and deveiling operators in order to process the task specific features efficiently where these operators address image formation formulation of these multiple degradations. FFT-op is motivated by Weiner deconvolution and help in learning the weights to efficiently fuse the task specific features and remove the effect of blur from the features. Deveiling operator is introduced to learn the weights in order to enhance low-light conditions efficiently. Furthermore, we use a classification network to classify the input degraded image into different classes that give information about the degradations that are present in the input face image. This class specific information is used as a prior information in the fusion network for fusing the task specific features. Fig. 1 shows sample results from the proposed Network Architecture Search for Face Enhancement (NASFE) method, where one can see that NASFE is able to provide better restoration results as compared to the state-of-the-art face restoration methods.

To summarize, this paper makes the following contributions:

- We propose a way of extracting the identity information from different clean images of a person present in the degraded image to restore the face image.
- We propose a novel loss, called identity-loss ( $\mathcal{L}_{iden}$ ), which uses the aforementioned identity information to train the NASFE network.
- We propose a neural architecture search-based method for designing the fusion network.

## 2. Related work

**Denosing.** Earlier methods such as [9, 93, 11, 17] make use of image priors to perform denosing. They require the knowledge about the amount of noise present in the noisy image to obtain denoised images. In contrast to these methods, blind image denosing methods like [90, 29, 38], model the noise using techniques like Non-local Bayes, and Low-rank mixture of Gaussians. CSF [61] and TDRN [7] proposed optimization algorithms in addressing stage-wise inference methods. The advent of convolutional networks in addressing image restoration problem allowed, DnCNN [87], FFDNet [85], RED30 [44], and BM3D-Net [79] to achieve impressive performance in denosing. Noise2Noise [30] method proposed a method that doesn't require paired noise-clean images to train the network. They rely on statistical reasoning and train the network using pairs of noisy images. Authors of CBDNet [19]

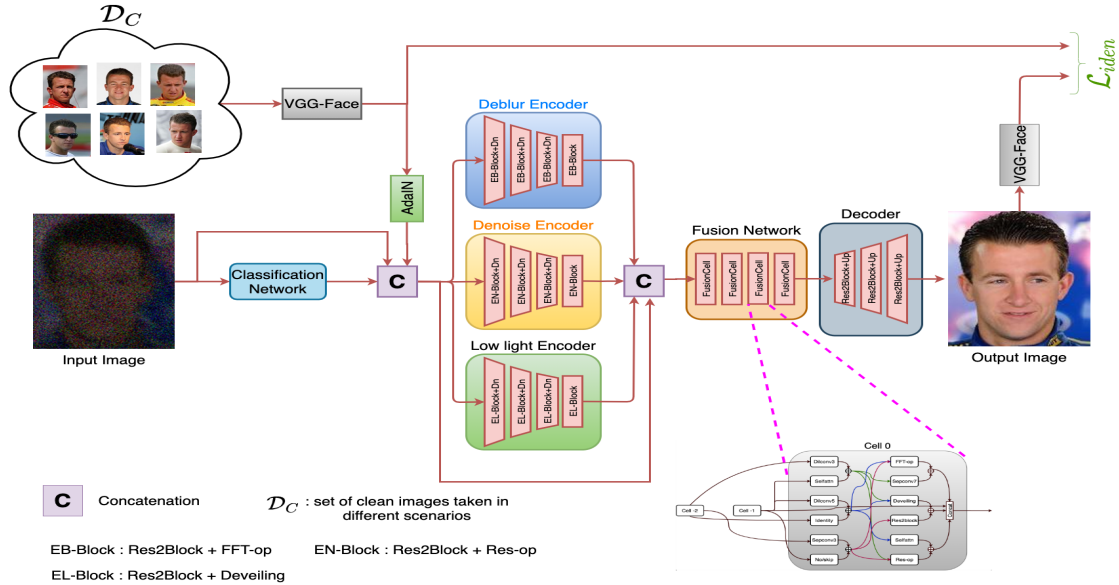


Figure 2: An overview of the proposed NASFE face image restoration network.

proposed an elegant way to model realistic noisy image, and use them to train the network that uses asymmetric learning to suppress under estimation of noise level.

**Deblurring.** Classical image deblurring methods follow estimation of blur kernel given a blurry image, and then use a deconvolution technique to obtain deblurred image. [77, 13, 25, 58, 64, 49, 68, 47, 52] methods have been proposed to compute different priors like sparsity,  $L_0$  gradient prior, patch prior, manifold prior, and low-rank prior, in order to compute blur kernel from the given blurry image. In recent years, neural network-based methods have also been proposed for deblurring [76, 59, 43, 66, 82], super-resolution [84, 6, 2, 36, 78, 69]. Deblurring methods are classified into blind and non-blind deblurring methods based on the usage of blur kernel information while restoring the image. Recent non-blind image deblurring methods like [5, 26, 63, 64, 62, 70] assume and use some knowledge about the blur kernel. Several face deblurring methods extract structural information in the form of facial fucdial or key points, face exemplar mask or semantic masks. Pan *et al.*[48] extract exemplar face images and use them as a global prior to estimate the blur kernel. Recently, [66, 67] proposed to use the semantic maps of a face to deblur the image. HiFaceGAN [80] addressed face restoration using a multi-stage semantic generation framework. DFD-Net [35] proposed a dictionary-based method to produce high-resolution face image.

**Low-light enhancement.** Various methods have been proposed in the literature for addressing low-light enhancement problem. Methods such as histogram equalization [54],

matching region templates [22], contrast statistics [60], bilateral learning [16], intermediate HDR supervision [81], reinforcement learning [50, 55], and adversarial [8, 23] have been proposed in the literature. [12, 65] view the inverse of low-light image as a hazy image in order to estimate a low-light enhanced image. Wei *et al.* [73] proposed a realistic noise formation model based on the characteristics of CMOS photosensors, to synthesize realistic low-light images. Guo *et al.* [18] proposed a zero reference-based method that uses pixel-wise high-order curves for dynamic range adjustment to enhance dark images.

**Network Architecture Search.** Neural Architecture Search methods focuses on automatically designing or constructing neural network architectures that are efficient in addressing a specific problem to achieve the optimal performance. Several architecture search methods have been proposed that use reinforcement learning [91, 3, 89] and evolutionary algorithms [57, 74, 40, 45]. Recent architecture search methods like [53, 92, 56] focus on searching the repeatable cell structure, while fixing the network level structure fixed. These methods are more efficient and computationally less expensive than the earlier methods. PNAS [39] proposed a progressive search strategy that notably reduces the computational cost. Motivated by [37, 41], we propose an efficient way to design our fusion network that fuses the task specific features in addressing the removal of multiple degradations like noise, blur, and enhancing the low-light conditions.

### 3. Proposed Method

An observed image  $y$ , with multiple degradations can be modeled as follows,

$$y = r \odot (k * x) + n, \quad (1)$$

where  $x$  is the clean image,  $r$  is the irradiance map,  $k$  is the blur kernel, and  $n$  is the additive noise. Here,  $*$  and  $\odot$  denote convolution and element wise multiplication operations, respectively. Figure 2 gives an overview of the proposed NASFE network which consists of three task specific encoders, a fusion network and a decoder. The deblur encoder ( $E_B(\cdot)$ ), denoise encoder ( $E_N(\cdot)$ ) and low-light encoder ( $E_L(\cdot)$ ) are trained to address the corresponding tasks of deblurring, denoising, and low-light enhancement, respectively. These encoders are used to extract task-specific features which are then fused using a network architecture search (NAS) based fusion block. Finally, the fused features are passed through the decoder network to restore the face image. Additionally, with help of a classification network, we determine what degradations are present in the input image, and use them as a prior information to the task specific encoders and the fusion network. Furthermore, to improve the quality and preserve the identity in the restored face image, we extract identity information from a set of clean images corresponding to the same identity present in the degraded image in the form of VGGFace features. We denote them as the identity information ( $I_{iden}$ ), and pass them as input along with the degraded image to the NASFE network to restore the face image. Besides using this identity information, we construct an identity loss  $\mathcal{L}_{iden}$  to train the NASFE network.

Due to space limitations, details regarding the task specific encoders, classification network and the decoder network are provided in the supplementary document.

#### 3.1. Fusion Network

As can be seen from Fig. 2, the task specific features are concatenated and then fed into the fusion network. Rather than using a simple  $1 \times 1$  convolution or a residual block to fuse these features, we proposed to use a NAS-based approach for designing the fusion network [53, 56, 41, 37]. We define fusion cell as a smallest repeatable module used to construct the fusion network (see Fig. 3). In our approach, the network search space includes both network level search (i.e. searching the connection between different fusion cells), and cell level search (i.e. exploring structure of the fusion cell).

**Fusion Cell Architecture.** We adopt the cell design structure of [37] to define a fusion cell (represented as  $Cell(\cdot)$ ) as a directed acyclic graph consisting of  $B$  blocks. Each block  $i$  in the  $l^{th}$  fusion cell  $F^l$  is a two tensors to one tensor mapping structure determined as a tuple of  $(I_1, I_2, O_1, O_2, M)$ , where  $I_1, I_2 \in \mathcal{I}_l$  are selections of the input tensors,  $O_1, O_2 \in \mathcal{O}$  are selections of the layer types

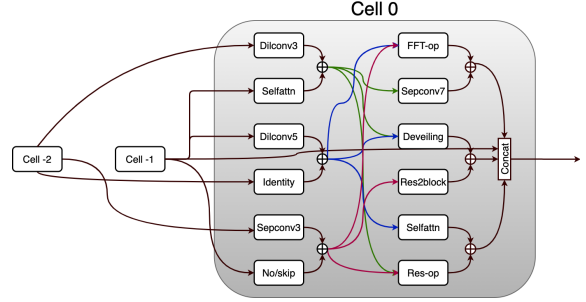


Figure 3: An illustration of the Fusion cell in the fusion network of NASFE. This figure shows a possible architectural layout of the fusion cell during training.

applied to the corresponding input tensors, and  $M \in \mathcal{M}$  is the method used to combine the outputs  $O_1, O_2$  to form the block  $F_i^l$ 's output tensor,  $Z_i^l$ . The fusion cell  $F^l$ 's output,  $Z^l$  is a concatenation of the outputs of all blocks  $\{Z_1^l, Z_2^l, \dots, Z_B^l\}$  in the cell  $F^l$ .  $\mathcal{I}_l$  is the set input tensor consisting of outputs of the previous cell  $F^{l-1}$  and previous-previous cell  $F^{l-2}$ . We follow [37], and use element wise addition as the only operator of possible combining method in  $\mathcal{M}$ . The set of possible layer types  $\mathcal{O}$  consist of the following ten operators:

- Dilconv3 (dilated conv3  $\times 3$ )
- Dilconv5 (dilated conv5  $\times 5$ )
- separable conv  $3 \times 3$
- separable conv  $5 \times 5$
- Identity or skip connection
- No or zero connection
- Selfattn (Self attention)
- Res2Block
- **Res-op (residual operator)**
- **Deveiling operator**
- **FFT operator**

Along with the conventional convolution operators like dilated, separable convolutions, no and skip connections, Res2Block [15] and self-attention block [71, 86], we introduce Res-op, deveiling and FFT-op (shown in Fig. 4) to efficiently process the task specific features. These operations are based on the image formation models regarding the individual degradation like noise, blur and low-light conditions. In what follows, we explain the design of these new operators in detail.

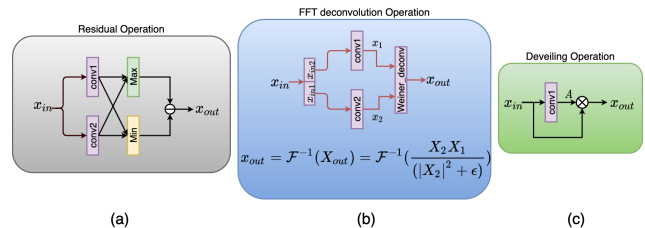


Figure 4: (a) Residual operator, (b) FFT-operator, (c) Deveiling operator. All the convblocks (conv1 and conv2) in these operators are  $3 \times 3$  convolutions.

**FFT operator.** Classical deblurring methods make use of the Wiener deconvolution technique to restore the image from blurry observations. Motivated by Wiener deconvolution, we split the features  $x_{in}$  into two parts  $x_{in1}$  and

$x_{in2}$ , and then apply convolution operation to obtain  $x_1$  and  $x_2$ , respectively. Finally, as shown in Fig. 4(b), we apply Weiner deconvolution to obtain  $x_{out} = \mathcal{F}^{-1}(X_{out})$ , where

$$X_{out} = \frac{X_2 X_1}{(|X_2|^2 + \epsilon)}. \quad (2)$$

Here,  $\mathcal{F}^{-1}$  denotes the inverse Fourier transform operator and  $X_1$ ,  $X_2$  and  $X_{out}$  are the Fourier transforms of  $x_1$ ,  $x_2$  and  $x_{out}$ , respectively. Here,  $\epsilon$  resembles the inverse of signal-to-noise ratio used during Weiner deconvolution which we set equal to 0.01.

**Deveiling operator.** [12, 65] viewed low-light enhancement as an image dehazing problem since both have similar mathematical models. [12] addressed low-light enhancement problem using a dark channel prior. Motivated by these methods, we use a deveiling operator [31, 34] to learn a latent mask  $A$  that enhances features from low-light conditions as follows

$$y = r \odot x + n \implies x = A \odot y, \quad (3)$$

where  $A = \frac{(y-n)^{ry}}{ry}$  is a learnable mask and a function of  $y$ . As shown in Fig. 4(c)  $A$  can be learned using a convolution layer given input features  $x_{in}$  and element wise multiplication of  $A$  with  $x_{in}$  to obtain the enhanced features  $x_{out}$ .

**Residual operator.** Inspired by the image deraining work [33] that uses a residual operator to remove rain streaks, we use a similar residual operator shown in Fig. 4(a) to estimate noise from the latent features and finally obtain noisy free features.

**Fusion Cell search space.** We use the continuous relaxation approach [40, 41] in which every output tensor  $Z_i^l$  of block  $F_i^l$  is connected to all input tensors  $I_i^l$  through operation  $O_{j \rightarrow i}$  as follows

$$Z_i^l = \sum_{Z_j^l \in I_i^l} O_{j \rightarrow i}(Z_j^l). \quad (4)$$

We define  $\bar{O}_{j \rightarrow i}$ , as approximation of the best search for operators  $O_{j \rightarrow i}$  using continuous relaxation as follows

$$\bar{O}_{j \rightarrow i}(Z_j^l) = \sum_{O^k \in \mathcal{O}} \alpha_{j \rightarrow i}^k O^k(Z_j^l), \quad (5)$$

where  $\sum_{k=1}^{|\mathcal{O}|} \alpha_{j \rightarrow i}^k = 1$ , and  $\alpha_{j \rightarrow i}^k \geq 0 \quad \forall i, j$ . This can be easily implemented using softmax. Hence, using Eq. 4 and Eq. 5, we can summarize the fusion cell architecture as follows,

$$Z^l = Cell(Z^{l-1}, Z^{l-2}, \alpha). \quad (6)$$

## 3.2. Identity Information

Given the degraded image  $y$ , and a set of clean images  $\mathcal{D}_C = \{C_i\}_{i=1}^n$ , we compute pool3 features using the VG-GFace network [51]. Note that  $\mathcal{D}_C$  contains clean images of the same person present in the degraded image  $y$ . Let  $F^y$  and  $\{F_i^C\}_{i=1}^n$  denote the VGGFace features corresponding

to  $y$  and  $\{C_i\}_{i=1}^n$ , respectively. Since the clean images in  $\mathcal{D}_C$  may have different style and characteristics as they may have been taken in different scenarios and times, we apply Adaptive-Instance normalization (AdaIN) before passing them as input to the network to reduce the effect of different styles in the images. AdaIN is applied as follows,

$$\bar{F}_i^C = \sigma(F^y) \left( \frac{F_i^C - \mu(F_i^C)}{\sigma(F_i^C)} \right) + \mu(F^y), \quad (7)$$

where  $\sigma(\cdot)$  and  $\mu(\cdot)$  denote standard deviation and mean, respectively. Mean of  $\bar{F}_i^C$  is defined as the identity information, i.e.  $I_{iden} = mean(\{\bar{F}_i^C\})$ .  $I_{iden}$  is used along with  $y$  as input to the NASFE network to restore the face image.

Note that as we are extracting the identity information from the clean images, this information is much more reliable and provides stronger prior as compared to face exemplar masks [48] or semantic maps [66, 2, 83] extracted using the degraded images. Additionally, to preserve the identity of the subject in restored image, we construct an identity loss  $\mathcal{L}_{iden}$  to train the NASFE network.

**Identity Loss  $\mathcal{L}_{iden}$ .** Let  $\hat{x}$  denote the restored face image using the NASFE network. We construct the identity loss as follows

$$\mathcal{L}_{iden} = \frac{1}{n} \sum_{i=1}^n \arccos(\langle F^{\hat{x}}, F_i^C \rangle), \quad (8)$$

where  $F^{\hat{x}}$  denotes the VGGFace features corresponding to  $\hat{x}$  and  $n$  denotes the number of clean images in  $\mathcal{D}_C$ .

## 3.3. Overall Loss

The NASFE network is trained using a combination of the L2 loss, perceptual loss [24] and identity loss as follows

$$\mathcal{L}_{final} = \mathcal{L}_2 + \lambda_{per} \mathcal{L}_{per} + \lambda_{iden} \mathcal{L}_{iden} \quad (9)$$

where  $\mathcal{L}_2 = \|\hat{x} - x\|_2^2$ ,  $\mathcal{L}_{iden}$  denotes the identity loss defined in (8) and  $\mathcal{L}_{per}$  denotes the perceptual loss [24] defined as follows

$$\mathcal{L}_{per} = \frac{1}{NHW} \sum_i \sum_j \sum_k \|F_{i,j,k}^{\hat{x}} - F_{i,j,k}^x\|. \quad (10)$$

Here,  $F^{\hat{x}}$ ,  $F^x$  denote the *pool3* layer features of the VG-GFace network [51] and  $N, H$  and  $W$  are the number of channels, height and width of  $F^{\hat{x}}$ , respectively. We set  $\lambda_{per} = 0.04$  and  $\lambda_{iden} = 0.003$  in our experiments.

Note that multiple clean images are required only during training. Once the network is trained, a degraded image is fed into the network and the NASFE produces identity-preserving restored image as the output.

## 4. NASFE Implementation Details

Given  $x$ , we first convolve it with  $k$  to get a blurry image. Here,  $k$  can be a motion blur kernel [1, 27] or an anisotropic Gaussian blur kernel [88]. To generate a degraded image with blur+low light+noise conditions, we fol-

Table 1: PSNR|SSIM comparisons against SOTA denoising methods using *Test-N*

Test-set		Noisy	BM3D [9] (TIP'7)	EPLL [93] (ICCV'11)	TNRD [7] (PAMI'16)	DnCNN [87] (TIP'17)	CBDNet [19] (CVPR'19)	NASFE (ours)
<i>Test-N</i>	CelebA	17.63 0.50	24.50 0.75	23.59 0.71	26.36 0.79	27.54 0.87	28.74 0.88	<b>29.23 0.90</b>
	VGGface2	18.52 0.46	24.45 0.73	23.87 0.73	26.91 0.81	27.71 0.88	28.88 0.89	<b>29.56 0.91</b>

Table 2: PSNR|SSIM comparisons against SOTA deblurring methods using *Test-B*

Test-set		Blurry	Pan <i>et al.</i> [48] (ECCV'14)	Super-FAN [2] (CVPR'18)	Shen <i>et al.</i> [66] (CVPR'19)	UMSN [83] (TIP'20)	DebluGAN-v2 [28] (ICCV'19)	HiFaceGAN [35] (ACMM'20)	NASFE (ours)
<i>Test-B</i>	CelebA	19.64 0.61	19.98 0.74	22.98 0.80	24.45 0.83	25.53 0.87	26.06 0.88	26.38 0.88	<b>27.90 0.92</b>
	VGGface2	20.30 0.67	20.74 0.77	22.83 0.80	24.63 0.84	25.65 0.87	25.92 0.87	26.30 0.88	<b>27.94 0.91</b>

Table 3: PSNR|SSIM comparisons against SOTA low-light enhancement methods using *Test-L*

Test set		Low-light	Fuet <i>et al.</i> [14] +DnCNN[87]	LIME[20] +DnCNN[87]	Liet <i>et al.</i> [32] +DnCNN[87]	Zero-DCE[18] +DnCNN[87]	Zero-DCE[18]+ ELD [73]	NASFE Ours
<i>Test-N</i>	CelebA	8.25 0.14	16.28 0.44	17.18 0.49	18.44 0.57	19.85 0.67	20.15 0.71	<b>23.04 0.80</b>
	VGGFace2	8.09 0.12	15.83 0.40	16.72 0.47	17.79 0.54	19.29 0.64	19.83 0.67	<b>22.94 0.79</b>

low [19, 73] and convert the obtained blurry image to irradiance image  $L$ . We then multiply low light factor  $r$  to  $L$ , where  $L = Mf^{-1}(k * x)$ ,  $f(\cdot)$  is the camera response function (CRF) function, and  $M(\cdot)$  represents the function that converts an RGB image to a Bayer image. Finally, we add realistic Photon-Gaussian noise [19], where  $n$  consists of two components: stationary noise  $n_c$  with noise variance  $\sigma_c^2$  and signal dependent noise  $n_s$  with spatially varying noise variance  $L\sigma_s^2$ .

**Training dataset.** We conduct our experiments using clean images from the CelebA [42] and VGGFace2 [4] face datasets. We randomly selected 30000 images from the training set of CelebA [42], and 30000 images from VGGFace2 [4] and generate synthetic degraded images with multiple degradations. Images in the CelebA and VGGFace2 datasets are of size  $176 \times 144$  and  $224 \times 224$ , respectively. Given a clean face image  $x$ , we first convolve it with blur kernel  $k$  sampled from 25000 motion kernels generated using [1, 27], and 8 anisotropic Gaussian kernels [88], and then following [73, 75] we multiply them with low light factor ( $r$ ) sampled uniformly from [0.05, 0.5] to obtain images with low-light conditions. Finally, we add realistic noise [19]  $n$  (where  $\sigma_s \in [0.01, 0.16]$  and  $\sigma_c \in [0.01, 0.06]$ ) to obtain the degraded image  $y$ . Based on the degradations present in  $y$ , we create class label  $c$  which is a vector of length three,  $c = \{b, n, l\}$  where  $b, n$ , and  $l$  are binary numbers, *i.e.*  $b, n$ , and  $l$  are one if  $y$  contains blur, noise and low-light, respectively and zero otherwise.

**Test datasets.** We create test datasets using randomly sampled 100 test images from the test sets of CelebA [42] and VGGFace2 [4]. Using these clean images, we create test datasets *Test-B*, *Test-N*, *Test-L*, *Test-BN*, and *Test-BNL* with the amounts of degradations as shown in the Table 4. Additionally, we collected a real-world face image dataset with multiple degradations corresponding to 20 subjects from

YouTube.

**Training Details.** The NASFE network is trained using Given  $\{y_i, x_i, c_i, \mathcal{D}_C^i\}_{i=1}^N$ . The classification network (CN) is trained using  $\{y_i, c_i\}_{i=1}^N$ . It is trained to produce a class label  $\hat{c}_i$  which indicates degradation(s) present in  $y_i$ .

Table 4: Details of the test datasets created using CelebA [51] and VGG-Face2 [4]. M: motion kernels [1], Gaussian: Gaussian kernels [88]

Test set name	Degradation type	Details about degradation values	Number of images	
			CelebA	VGGFace2
<i>Test-B</i>	blur	M: 40 kernels kernel size [13, 27] G: 12 anisotropic kernels with $\sigma_s \in [1, 3]$	5200	5200
<i>Test-N</i>	noise	$\sigma_s = [0.05, 0.1, 0.05]$ , $\sigma_c = [0.05, 0.1]$	600	600
<i>Test-L</i>	low-light	$r = [0.1, 0.15, 0.2, 0.25, 0.3, 0.35]$ $\sigma_s = [0.05, 0.1]$ , $\sigma_c = [0.05, 0.1]$	2400	2400
<i>Test-BN</i>	blur + noise	M: 40 kernels kernel size [13, 27] G: 12 anisotropic kernels with $\sigma_s \in [1, 3]$ $\sigma_s = 0.1$ , $\sigma_c = 0.05$	10400	10400
<i>Test-BNL</i>	blur + noise + low-light	M: 40 kernels kernel size [13, 27] G: 12 anisotropic kernels with $\sigma_s \in [1, 3]$ $r = [0.15, 0.3]$ , $\sigma_s = 0.1$ , $\sigma_c = 0.05$	10400	10400

Training and network details of the classification network are provided in the supplementary document. NASFE contains three encoders (deblur ( $E_B(\cdot)$ ), denoise ( $E_N(\cdot)$ ) and low-light ( $E_L(\cdot)$ )), one fusion network ( $F_n(\cdot)$ ) and a decoder ( $De(\cdot)$ ). Encoders ( $E_B, E_N, E_L$ ) are initially trained to address the corresponding individual tasks of deblurring, denoising, and low-light enhancement, respectively. More details are provided in the supplementary document. Given a degraded image  $y$ , we compute class  $\hat{c}$  (using CN) and identity information  $I_{iden}$  and pass them as input to NASFE to compute a restored image  $\hat{x}$ . We set the number of blocks  $B$  to 12 in the Fusion cell of NASFE. Following [37], we update  $\alpha$  and the weights of the NASFE alternately during training. NASFE is trained using  $\mathcal{L}^{final}$  with the Adam optimizer and batch size of 40. The learning rate is set equal to 0.0005. NASFE is trained for one million

iterations.

## 5. Experiments and Results

We compare the performance of our network against the state-of-the-art (SOTA) denoising [9, 93, 7, 87, 19], deblurring [48, 2, 66, 83, 28, 35, 80], and low-light enhancement methods [14, 20, 32, 18, 73]. Peak-Signal-to-Noise Ratio (PSNR) and Structural Similarity index (SSIM) [72] measures are used to compare the performance of different methods on synthetic images. Note that we retrain the SOTA methods [2, 66, 83, 28, 35, 80] using the training data discussed earlier and following the procedures explained in the respective papers. Additionally, we provide visual comparisons of NASFE against the SOTA methods using the real blurry images provided by [66], and real low-light exposure images published by [18, 3].

### 5.1. Single degradation experiments

**Denoising Experiments.** We perform quantitative analysis of NASFE against the SOTA denoising methods [9, 93, 7, 87, 19] using *Test-N*. As can be seen from Table 1, our method outperformed the SOTA method by 0.6dB in PSNR and 0.02 in SSIM. Note that methods such as [87, 19] are specifically designed for image denoising. Even though our method is designed for dealing with multiple degradations, it provides better performance than SOTA denoising methods.

**Deblurring Experiments.** We compare the performance of NASFE against SOTA deblurring [48, 46, 2, 66, 83, 28] methods using *Test-B*. Methods such as [48, 46, 2, 66, 83] use facial exemplar or semantic information as priors to perform deblurring. On the other hand, our network uses identity information as a prior to perform deblurring. As can be seen from Table 2, our method outperforms the SOTA method by 1.93dB in PSNR and 0.04 in SSIM.

**Low-light Enhancement Experiments.** We evaluated the performance of NASFE against SOTA low-light enhancement methods [14, 20, 32, 18, 73] using *Test-L*. Even though our method is trained for addressing multiple degradations, NASFE performed significantly better than [14, 20, 32, 18, 73]. As can be seen from Table 3, our method outperforms SOTA methods [14, 20, 32, 18, 73] by 3dB in PSNR and 0.10 in SSIM.

More qualitative results are provided in the supplementary document.

### 5.2. Multiple degradation experiments

**Blur + Noise + Low-light Experiments.** We compare the performance of different methods on *Test-BNL* which contains multiple degradations blur, noise, and low-light conditions. Note, we retrain [2, 66, 83, 28, 35, 80] using degraded

images that contain all degradations. Results are corresponding to this experiment are shown in Table 5. As can be seen from this table, NASFE performs better by 2.1dB in PSNR and 0.07 in SSIM compared to second best performing method. Fig. 5 shows the qualitative results of NASFE against other methods. The outputs of other methods are blurry or contain artifacts near eyes, nose and mouth. On the other hand, NASFE produces clear and sharp face images. Furthermore, we can observe from Fig. 5 and Fig. 6 that outputs of other methods still contain low-light conditions, whereas NASFE produces sharp face images with enhanced lighting conditions.

We conducted face recognition experiments using *Test-BNL*, to show the significance of various face restoration methods on face recognition. Face recognition experiments are conducted using ArcFace [10] on *Test-BN*, where Top-K similar faces for the restored face image are picked from the gallery set and used to compute accuracy. Table 5 show the face recognition accuracies corresponding to different methods. We can clearly see that NASFE achieves an improvement of 7% over the second best performing method.

### 5.3. Ablation study

We conduct ablation studies using the test-sets *Test-BN*, and *Test-BNL* to show the improvements achieved by the different components in NASFE. We start with the baseline network (BN), and define it as a combination of three encoders ( $E_B$ ,  $E_N$ , and  $E_L$ ), a fusion network (composed of 4 Res2Blocks [15]), and a decoder ( $De$ ). As shown in Table 6, BN performs very poorly due to its inability in processing task-specific features efficiently. Now, we introduce network architecture search in the fusion network by using fusion cells in-order to efficiently processing the task-specific features. The use of network architecture search results in improvement of BN-NAS by  $\sim 2$ dB compared to BN. Then, we use class labels  $c$  (computed using classification network) as input to BN-NAS which increases the performance of the network by  $\sim 0.5$ dB. Now we use the proposed identity information  $I_{iden}$  of the identity present in the degraded image (refer to section 3.2) which further improves the performance of the network by  $\sim 1.5$ dB. The resultant network corresponds to NASFE. Note that BN and BN-NAS are trained using  $\mathcal{L}_{mse}$ . Now we train NASFE with  $\mathcal{L}_{mse}$  and  $\mathcal{L}_{per}$  which further improves the performance by 0.3dB. Now we use the proposed  $\mathcal{L}_{iden}$  to construct  $\mathcal{L}_{final}$  and train NASFE. The proposed  $\mathcal{L}_{iden}$  improves the performance of NASFE by  $\sim 0.5$ dB.

## 6. Conclusion

We proposed a multi-task face restoration network, called NASFE, that can enhance poor quality face images containing a single degradation (i.e. noise or blur) or multiple degradations (noise+blur+low-light). NASFE makes

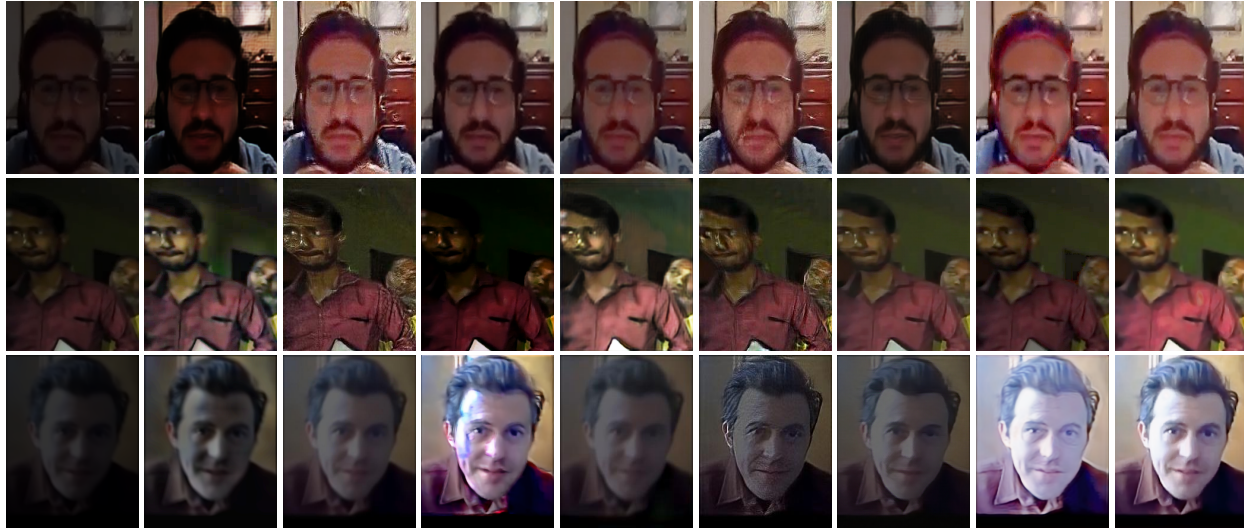


Figure 5: Qualitative comparisons using real face images multiple degradations collected from YouTube videos. output images of Histeq are computed using Histogram equalization method.



Figure 6: Qualitative comparisons using synthetic test set *Test-BNL*, B:blur, N: noise, L: low-light condition.

Table 5: PSNR|SSIM and face recognition comparisons of NASFE using *Test-BNL*. B: blur, N: noise, L: low-light. (Note all methods are retrained using degraded images containing blur, noise and low-light conditions. Histeq means Histogram equalization method)

Test-set	Metrics	B+N+L	Histeq	Shen et al. [66] (CVPR'18)	Super-FAN [2] (CVPR'18)	UMSN [83] (TIP'20)	DeblurGANv2 [28] (ICCV'19)	DFDNet [28] (ECCV'20)	HiFaceGAN [28] (ACMM'20)	NASFE w/o $I_{den}$	NASFE (ours)	
Test-BNL	CelebA	PSNR SSIM	8.17 0.22	12.28 0.39	19.98 0.66	19.45 0.60	21.10  0.72	21.37 0.74	21.68 0.77	21.75 0.77	22.53 0.81	<b>23.80 0.85</b>
		Top-1 Top-5	38.5 45.2	41.3 47.5	51.2 57.8	48.8 55.9	59.7 67.7	61.2   68.6	63.4 69.7	62.9 69.1	69.6 77.3	<b>73.4 81.8</b>
	VGGFace2	PSNR SSIM	8.39 0.25	12.84 0.41	20.46 0.68	19.83 0.64	21.28  0.72	21.94 0.78	21.96 0.78	22.08 0.79	22.84 0.83	<b>24.15 0.86</b>
		Top-1 Top-5	42.8 49.2	43.2 50.8	56.9 62.7	53.8 59.2	62.8  69.9	65.3 72.4	67.8 73.7	67.2 72.9	72.1 80.4	<b>75.9 84.2</b>

use of the clean face images of a person present in the degraded image to extract the identity information, and uses it to train the network weights. Additionally, we use network architecture search to design the fusion network in NASFE that fuses the task-specific features obtained from

the encoders. Extensive experiments shows that the proposed method performance significantly better than SOTA image restoration/enhancement methods on both synthetic degraded images as well as real-world images with multiple degradations (noise+blur+low-light).



Table 6: PSNR|SSIM comparisons for ablation study using *Test-BN*, *Test-BNL*. Learnable parameters are in millions.

Method	<i>Test-BN</i>		<i>Test-BNL</i>		Learnable Parameters
	CelebA	VGGFace2	CelebA	VGGFace2	
baseline network (BN)	19.72 0.70	19.88 0.72	19.95 0.65	20.42 0.69	6.00
BN-NAS	22.51 0.74	22.62 0.75	21.17 0.70	21.47 0.74	6.25
+ classification network	23.28 0.76	23.04 0.76	21.56 0.72	21.95 0.76	6.25
+ identity information $\mathcal{L}_{iden}$	24.88 0.81	24.60 0.82	23.06 0.80	23.47 0.80	6.40
NASFE (w/ $\mathcal{L}_{mse}$ and $\mathcal{L}_{per}$ )	25.10 0.84	24.92 0.84	23.35 0.83	23.76 0.83	6.40
NASFE w/ $\mathcal{L}_{final}$	25.57 0.87	25.49 0.87	23.80 0.85	24.15 0.86	6.40

## References

- [1] Giacomo Boracchi and Alessandro Foi. Modeling the performance of image restoration from motion blur. *IEEE Transactions on Image Processing*, 21(8):3502–3517, 2012. 5, 6
- [2] Adrian Bulat and Georgios Tzimiropoulos. Super-fan: Integrated facial landmark localization and super-resolution of real-world low resolution faces in arbitrary poses with gans. In *Proceedings of the IEEE Conference on Computer Vision and Pattern Recognition*, pages 109–117, 2018. 1, 2, 3, 5, 6, 7, 8
- [3] Han Cai, Tianyao Chen, Weinan Zhang, Yong Yu, and Jun Wang. Efficient architecture search by network transformation. *arXiv preprint arXiv:1707.04873*, 2017. 3, 7
- [4] Qiong Cao, Li Shen, Weidi Xie, Omkar M Parkhi, and Andrew Zisserman. Vggface2: A dataset for recognising faces across pose and age. In *2018 13th IEEE International Conference on Automatic Face & Gesture Recognition (FG 2018)*, pages 67–74. IEEE, 2018. 6
- [5] Ayan Chakrabarti. Deep convolutional neural network for image deconvolution. 2014. 3
- [6] Dongdong Chen, Mingming He, Qingnan Fan, Jing Liao, Liheng Zhang, Dongdong Hou, Lu Yuan, and Gang Hua. Gated context aggregation network for image dehazing and deraining. pages 1375–1383, 2019. 3
- [7] Yunjin Chen and Thomas Pock. Trainable nonlinear reaction diffusion: A flexible framework for fast and effective image restoration. *IEEE transactions on pattern analysis and machine intelligence*, 39(6):1256–1272, 2016. 2, 6, 7
- [8] Yu-Sheng Chen, Yu-Ching Wang, Man-Hsin Kao, and Yung-Yu Chuang. Deep photo enhancer: Unpaired learning for image enhancement from photographs with gans. In *Proceedings of the IEEE Conference on Computer Vision and Pattern Recognition (CVPR)*, June 2018. 3
- [9] Kostadin Dabov, Alessandro Foi, Vladimir Katkovnik, and Karen Egiazarian. Image denoising by sparse 3-d transform-domain collaborative filtering. *IEEE Transactions on image processing*, 16(8):2080–2095, 2007. 2, 6, 7
- [10] Jiankang Deng, Jia Guo, Niannan Xue, and Stefanos Zafeiriou. Arcface: Additive angular margin loss for deep face recognition. In *Proceedings of the IEEE Conference on Computer Vision and Pattern Recognition*, pages 4690–4699, 2019. 7
- [11] Weisheng Dong, Lei Zhang, Guangming Shi, and Xin Li. Nonlocally centralized sparse representation for image restoration. *IEEE transactions on Image Processing*, 22(4):1620–1630, 2012. 2
- [12] D. L. Donoho and M. E. Raimondo. A fast wavelet algorithm for image deblurring. In Rob May and A. J. Roberts, editors, *Proc. of 12th Computational Techniques and Applications Conference CTAC-2004*, volume 46, pages C29–C46, Mar. 2005. <http://anziamj.austms.org.au/V46/CTAC2004/Dono>. 3, 5
- [13] Rob Fergus, Barun Singh, Aaron Hertzmann, Sam T Roweis, and William T Freeman. Removing camera shake from a single photograph. *ACM transactions on graphics (TOG)*, 25(3):787–794, 2006. 3
- [14] Xueyang Fu, Delu Zeng, Yue Huang, Xiao-Ping Zhang, and Xinghao Ding. A weighted variational model for simultaneous reflectance and illumination estimation. In *Proceedings of the IEEE Conference on Computer Vision and Pattern Recognition*, pages 2782–2790, 2016. 6, 7
- [15] Shanghua Gao, Ming-Ming Cheng, Kai Zhao, Xin-Yu Zhang, Ming-Hsuan Yang, and Philip HS Torr. Res2net: A new multi-scale backbone architecture. *IEEE transactions on pattern analysis and machine intelligence*, 2019. 2, 4, 7
- [16] Michaël Gharbi, Jiawen Chen, Jonathan T Barron, Samuel W Hasinoff, and Frédéric Durand. Deep bilateral learning for real-time image enhancement. *ACM Transactions on Graphics (TOG)*, 36(4):1–12, 2017. 3
- [17] Shuhang Gu, Lei Zhang, Wangmeng Zuo, and Xiangchu Feng. Weighted nuclear norm minimization with application to image denoising. In *Proceedings of the IEEE conference on computer vision and pattern recognition*, pages 2862–2869, 2014. 2
- [18] Chunle Guo, Chongyi Li, Jichang Guo, Chen Change Loy, Junhui Hou, Sam Kwong, and Runmin Cong. Zero-reference deep curve estimation for low-light image enhancement. In *Proceedings of the IEEE/CVF Conference on Computer Vision and Pattern Recognition*, pages 1780–1789, 2020. 3, 6, 7
- [19] Shi Guo, Zifei Yan, Kai Zhang, Wangmeng Zuo, and Lei Zhang. Toward convolutional blind denoising of real photographs. In *Proceedings of the IEEE Conference on Computer Vision and Pattern Recognition*, pages 1712–1722, 2019. 2, 6, 7
- [20] Xiaojie Guo, Yu Li, and Haibin Ling. Lime: Low-light image enhancement via illumination map estimation. *IEEE Transactions on image processing*, 26(2):982–993, 2016. 6, 7
- [21] Xun Huang and Serge Belongie. Arbitrary style transfer in real-time with adaptive instance normalization. In *Proceedings of the IEEE International Conference on Computer Vision*, pages 1501–1510, 2017. 2
- [22] Sung Ju Hwang, Ashish Kapoor, and Sing Bing Kang. Context-based automatic local image enhancement. In *European conference on computer vision*, pages 569–582. Springer, 2012. 3
- [23] Andrey Ignatov, Nikolay Kobyshev, Radu Timofte, Kenneth Vanhoey, and Luc Van Gool. Dslr-quality photos on mobile devices with deep convolutional networks. In *Proceedings of the IEEE International Conference on Computer Vision*, pages 3277–3285, 2017. 3

- [24] Justin Johnson, Alexandre Alahi, and Li Fei-Fei. Perceptual losses for real-time style transfer and super-resolution. *ECCV*, 2016. 5
- [25] Dilip Krishnan, Terence Tay, and Rob Fergus. Blind deconvolution using a normalized sparsity measure. *CVPR 2011*, pages 233–240, 2011. 3
- [26] Jakob Kruse, Carsten Rother, and Uwe Schmidt. Learning to push the limits of efficient fft-based image deconvolution. In *Proceedings of the IEEE International Conference on Computer Vision*, pages 4586–4594, 2017. 3
- [27] Orest Kupyn, Volodymyr Budzan, Mykola Mykhailych, Dmytro Mishkin, and Jiří Matas. Deblurgan: Blind motion deblurring using conditional adversarial networks. In *Proceedings of the IEEE conference on computer vision and pattern recognition*, pages 8183–8192, 2018. 5, 6
- [28] Orest Kupyn, Tetiana Martyniuk, Junru Wu, and Zhangyang Wang. Deblurgan-v2: Deblurring (orders-of-magnitude) faster and better. In *Proceedings of the IEEE International Conference on Computer Vision*, pages 8878–8887, 2019. 1, 6, 7, 8
- [29] Marc Lebrun, Miguel Colom, and Jean-Michel Morel. Multiscale image blind denoising. *IEEE Transactions on Image Processing*, 24(10):3149–3161, 2015. 2
- [30] Jaakko Lehtinen, Jacob Munkberg, Jon Hasselgren, Samuli Laine, Tero Karras, Miika Aittala, and Timo Aila. Noise2noise: Learning image restoration without clean data. *arXiv preprint arXiv:1803.04189*, 2018. 2
- [31] Boyi Li, Xiulian Peng, Zhangyang Wang, Jizheng Xu, and Dan Feng. Aod-net: All-in-one dehazing network. In *Proceedings of the IEEE international conference on computer vision*, pages 4770–4778, 2017. 5
- [32] Mading Li, Jiaying Liu, Wenhan Yang, Xiaoyan Sun, and Zongming Guo. Structure-revealing low-light image enhancement via robust retinex model. *IEEE Transactions on Image Processing*, 27(6):2828–2841, 2018. 6, 7
- [33] Ruoteng Li, Robby T Tan, and Loong-Fah Cheong. Robust optical flow in rainy scenes. In *Proceedings of the European Conference on Computer Vision (ECCV)*, pages 288–304, 2018. 5
- [34] Ruoteng Li, Robby T Tan, Loong-Fah Cheong, Angelica I Aviles-Rivero, Qingnan Fan, and Carola-Bibiane Schonlieb. Rainflow: Optical flow under rain streaks and rain veiling effect. In *Proceedings of the IEEE International Conference on Computer Vision*, pages 7304–7313, 2019. 5
- [35] Xiaoming Li, Chaofeng Chen, Shangchen Zhou, Xianhui Lin, Wangmeng Zuo, and Lei Zhang. Blind face restoration via deep multi-scale component dictionaries. In *ECCV*, 2020. 1, 2, 3, 6, 7, 8
- [36] Xiaoming Li, Wenyu Li, Dongwei Ren, Hongzhi Zhang, Meng Wang, and Wangmeng Zuo. Enhanced blind face restoration with multi-exemplar images and adaptive spatial feature fusion. In *CVPR*, 2020. 2, 3
- [37] Chenxi Liu, Liang-Chieh Chen, Florian Schroff, Hartwig Adam, Wei Hua, Alan L Yuille, and Li Fei-Fei. Auto-deeplab: Hierarchical neural architecture search for semantic image segmentation. In *Proceedings of the IEEE conference on computer vision and pattern recognition*, pages 82–92, 2019. 3, 4, 6
- [38] Ce Liu, Richard Szeliski, Sing Bing Kang, C Lawrence Zitnick, and William T Freeman. Automatic estimation and removal of noise from a single image. *IEEE transactions on pattern analysis and machine intelligence*, 30(2):299–314, 2007. 2
- [39] Chenxi Liu, Barret Zoph, Maxim Neumann, Jonathon Shlens, Wei Hua, Li-Jia Li, Li Fei-Fei, Alan Yuille, Jonathan Huang, and Kevin Murphy. Progressive neural architecture search. In *Proceedings of the European Conference on Computer Vision (ECCV)*, pages 19–34, 2018. 3
- [40] Hanxiao Liu, Karen Simonyan, Oriol Vinyals, Chrisantha Fernando, and Koray Kavukcuoglu. Hierarchical representations for efficient architecture search. *arXiv preprint arXiv:1711.00436*, 2017. 2, 3, 5
- [41] Hanxiao Liu, Karen Simonyan, and Yiming Yang. Darts: Differentiable architecture search. *arXiv preprint arXiv:1806.09055*, 2018. 2, 3, 4, 5
- [42] Ziwei Liu, Ping Luo, Xiaogang Wang, and Xiaoou Tang. Deep learning face attributes in the wild. In *Proceedings of the IEEE international conference on computer vision*, pages 3730–3738, 2015. 6
- [43] Boyu Lu, Jun-Cheng Chen, and Rama Chellappa. Unsupervised domain-specific deblurring via disentangled representations. In *Proceedings of the IEEE Conference on Computer Vision and Pattern Recognition*, pages 10225–10234, 2019. 3
- [44] Xiaojiao Mao, Chunhua Shen, and Yu-Bin Yang. Image restoration using very deep convolutional encoder-decoder networks with symmetric skip connections. In *Advances in neural information processing systems*, pages 2802–2810, 2016. 2
- [45] Risto Mäikkulainen, Jason Liang, Elliot Meyerson, Aditya Rawal, Daniel Fink, Olivier Francon, Bala Raju, Hormoz Shahrzad, Arshak Navruzyan, Nigel Duffy, et al. Evolving deep neural networks. In *Artificial Intelligence in the Age of Neural Networks and Brain Computing*, pages 293–312. Elsevier, 2019. 3
- [46] Seungjun Nah, Tae Hyun Kim, and Kyoung Mu Lee. Deep multi-scale convolutional neural network for dynamic scene deblurring. In *Proceedings of the IEEE Conference on Computer Vision and Pattern Recognition*, pages 3883–3891, 2017. 7
- [47] J. Ni, P. Turaga, V. M. Patel, and R. Chellappa. Example-driven manifold priors for image deconvolution. *IEEE Transactions on Image Processing*, 20(11):3086–3096, Nov 2011. 3
- [48] Jinshan Pan, Zhe Hu, Zhixun Su, and Ming-Hsuan Yang. Deblurring face images with exemplars. pages 47–62, 2014. 1, 2, 3, 5, 6, 7
- [49] Jinshan Pan, Deqing Sun, Hanspeter Pfister, and Ming-Hsuan Yang. Blind image deblurring using dark channel prior. In *Proceedings of the IEEE Conference on Computer Vision and Pattern Recognition*, pages 1628–1636, 2016. 3
- [50] Jongchan Park, Joon-Young Lee, Donggeun Yoo, and In So Kweon. Distort-and-recover: Color enhancement using deep reinforcement learning. In *Proceedings of the IEEE Conference on Computer Vision and Pattern Recognition*, pages 5928–5936, 2018. 3

- [51] O. M. Parkhi, A. Vedaldi, and A. Zisserman. Deep face recognition. In *British Machine Vision Conference*, 2015. 2, 5, 6
- [52] V. M. Patel, G. R. Easley, and D. M. Healy. Shearlet-based deconvolution. *IEEE Transactions on Image Processing*, 18(12):2673–2685, Dec 2009. 3
- [53] Hieu Pham, Melody Y Guan, Barret Zoph, Quoc V Le, and Jeff Dean. Efficient neural architecture search via parameter sharing. *arXiv preprint arXiv:1802.03268*, 2018. 3, 4
- [54] Stephen M Pizer, E Philip Amburn, John D Austin, Robert Cromartie, Ari Geselowitz, Trey Greer, Bart ter Haar Romeny, John B Zimmerman, and Karel Zuiderveld. Adaptive histogram equalization and its variations. *Computer vision, graphics, and image processing*, 39(3):355–368, 1987. 3
- [55] A. Ramirez Rivera, Byungyong Ryu, and O. Chae. Content-aware dark image enhancement through channel division. *IEEE Transactions on Image Processing*, 21(9):3967–3980, 2012. 3
- [56] Esteban Real, Alok Aggarwal, Yanping Huang, and Quoc V Le. Regularized evolution for image classifier architecture search. In *Proceedings of the aaai conference on artificial intelligence*, volume 33, pages 4780–4789, 2019. 3, 4
- [57] Esteban Real, Sherry Moore, Andrew Selle, Saurabh Saxena, Yutaka Leon Suematsu, Jie Tan, Quoc Le, and Alex Kurakin. Large-scale evolution of image classifiers. *arXiv preprint arXiv:1703.01041*, 2017. 3
- [58] Wenqi Ren, Xiaochun Cao, Jinshan Pan, Xiaojie Guo, Wangmeng Zuo, and Ming-Hsuan Yang. Image deblurring via enhanced low-rank prior. *IEEE Transactions on Image Processing*, 25(7):3426–3437, 2016. 3
- [59] Wenqi Ren, Jiaolong Yang, Senyou Deng, David Wipf, Xiaochun Cao, and Xin Tong. Face video deblurring using 3d facial priors. In *Proceedings of the IEEE International Conference on Computer Vision*, pages 9388–9397, 2019. 3
- [60] Adin Ramirez Rivera, Byungyong Ryu, and Oksam Chae. Content-aware dark image enhancement through channel division. *IEEE transactions on image processing*, 21(9):3967–3980, 2012. 3
- [61] Uwe Schmidt and Stefan Roth. Shrinkage fields for effective image restoration. In *Proceedings of the IEEE conference on computer vision and pattern recognition*, pages 2774–2781, 2014. 2
- [62] Uwe Schmidt and Stefan Roth. Shrinkage fields for effective image restoration. In *Proceedings of the IEEE Conference on Computer Vision and Pattern Recognition*, pages 2774–2781, 2014. 3
- [63] Uwe Schmidt, Carsten Rother, Sebastian Nowozin, Jeremy Jancsary, and Stefan Roth. Discriminative non-blind deblurring. In *Proceedings of the IEEE Conference on Computer Vision and Pattern Recognition*, pages 604–611, 2013. 3
- [64] Christian J Schuler, Harold Christopher Burger, Stefan Harmeling, and Bernhard Scholkopf. A machine learning approach for non-blind image deconvolution. In *Proceedings of the IEEE Conference on Computer Vision and Pattern Recognition*, pages 1067–1074, 2013. 3
- [65] Pradeep Sen, Nima Khademi Kalantari, Maziar Yaesoubi, Soheil Darabi, Dan B Goldman, and Eli Shechtman. Robust Patch-Based HDR Reconstruction of Dynamic Scenes. *ACM Transactions on Graphics (TOG) (Proceedings of SIGGRAPH Asia 2012)*, 31(6):203:1–203:11, 2012. 3, 5
- [66] Ziyi Shen, Wei-Sheng Lai, Tingfa Xu, Jan Kautz, and Ming-Hsuan Yang. Deep semantic face deblurring. *Proceedings of the IEEE Conference on Computer Vision and Pattern Recognition*, pages 8260–8269, 2018. 1, 2, 3, 5, 6, 7, 8
- [67] Ziyi Shen, Wei-Sheng Lai, Tingfa Xu, Jan Kautz, and Ming-Hsuan Yang. Exploiting semantics for face image deblurring. *International Journal of Computer Vision*, 2020. 3
- [68] Libin Sun, Sunghyun Cho, Jue Wang, and James Hays. Edge-based blur kernel estimation using patch priors. In *IEEE International Conference on Computational Photography (ICCP)*, pages 1–8. IEEE, 2013. 3
- [69] Hamid Vaezi Joze, Ilya Zharkov, Karlton Powell, Carl Ringler, Luming Liang, Andy Roulston, Moshe Lutz, and Vivek Pradeep. Imagepairs: Realistic super resolution dataset via beam splitter camera rig. In *The IEEE Conference on Computer Vision and Pattern Recognition (CVPR) Workshops*, 2020. 3
- [70] Subeesh Vasu, Venkatesh Reddy Maligireddy, and AN Rajagopalan. Non-blind deblurring: Handling kernel uncertainty with cnns. In *Proceedings of the IEEE Conference on Computer Vision and Pattern Recognition*, pages 3272–3281, 2018. 3
- [71] Ashish Vaswani, Noam Shazeer, Niki Parmar, Jakob Uszkoreit, Llion Jones, Aidan N Gomez, Łukasz Kaiser, and Illia Polosukhin. Attention is all you need. In *Advances in neural information processing systems*, pages 5998–6008, 2017. 4
- [72] Zhou Wang, Alan C Bovik, Hamid R Sheikh, and Eero P Simoncelli. Image quality assessment: from error visibility to structural similarity. *IEEE transactions on image processing*, 13(4):600–612, 2004. 7
- [73] Kaixuan Wei, Ying Fu, Jiaolong Yang, and Hua Huang. A physics-based noise formation model for extreme low-light raw denoising. In *Proceedings of the IEEE/CVF Conference on Computer Vision and Pattern Recognition*, pages 2758–2767, 2020. 3, 6, 7
- [74] Lingxi Xie and Alan Yuille. Genetic cnn. In *Proceedings of the IEEE international conference on computer vision*, pages 1379–1388, 2017. 3
- [75] Ke Xu, Xin Yang, Baocai Yin, and Rynson WH Lau. Learning to restore low-light images via decomposition-and-enhancement. In *Proceedings of the IEEE/CVF Conference on Computer Vision and Pattern Recognition*, pages 2281–2290, 2020. 6
- [76] Li Xu, Jimmy SJ Ren, Ce Liu, and Jiaya Jia. Deep convolutional neural network for image deconvolution. In *Advances in neural information processing systems*, pages 1790–1798, 2014. 3
- [77] Li Xu, Shicheng Zheng, and Jiaya Jia. Unnatural l0 sparse representation for natural image deblurring. *Proceedings of the IEEE conference on computer vision and pattern recognition*, pages 1107–1114, 2013. 3

- [78] Xiangyu Xu, Deqing Sun, Jinshan Pan, Yujin Zhang, Hanspeter Pfister, and Ming-Hsuan Yang. Learning to super-resolve blurry face and text images. In *Proceedings of the IEEE international conference on computer vision*, pages 251–260, 2017. [3](#)
- [79] Dong Yang and Jian Sun. Bm3d-net: A convolutional neural network for transform-domain collaborative filtering. *IEEE Signal Processing Letters*, 25(1):55–59, 2017. [2](#)
- [80] Lingbo Yang, C. Liu, P. Wang, Shanshe Wang, P. Ren, Siwei Ma, and W. Gao. Hifacegan: Face renovation via collaborative suppression and replenishment. *Proceedings of the 28th ACM International Conference on Multimedia*, 2020. [1](#), [2](#), [3](#), [7](#), [8](#)
- [81] Xin Yang, Ke Xu, Yibing Song, Qiang Zhang, Xiaopeng Wei, and Rynson WH Lau. Image correction via deep reciprocating hdr transformation. In *Proceedings of the IEEE Conference on Computer Vision and Pattern Recognition*, pages 1798–1807, 2018. [3](#)
- [82] Rajeev Yasarla and Vishal M Patel. Learning to restore a single face image degraded by atmospheric turbulence using cnns. *arXiv preprint arXiv:2007.08404*, 2020. [3](#)
- [83] Rajeev Yasarla, Federico Perazzi, and Vishal M Patel. Deblurring face images using uncertainty guided multi-stream semantic networks. *IEEE Transactions on Image Processing*, 29:6251–6263, 2020. [1](#), [2](#), [5](#), [6](#), [7](#), [8](#)
- [84] Xin Yu, Basura Fernando, Bernard Ghanem, Fatih Porikli, and Richard Hartley. Face super-resolution guided by facial component heatmaps. In *Proceedings of the European Conference on Computer Vision (ECCV)*, pages 217–233, 2018. [3](#)
- [85] Hang Zhang and Kristin Dana. Multi-style generative network for real-time transfer. *arXiv preprint arXiv:1703.06953*, 2017. [2](#)
- [86] Han Zhang, Ian Goodfellow, Dimitris Metaxas, and Augustus Odena. Self-attention generative adversarial networks. In *International Conference on Machine Learning*, pages 7354–7363. PMLR, 2019. [4](#)
- [87] Kai Zhang, Wangmeng Zuo, Yunjin Chen, Deyu Meng, and Lei Zhang. Beyond a gaussian denoiser: Residual learning of deep cnn for image denoising. *IEEE Transactions on Image Processing*, 26(7):3142–3155, 2017. [2](#), [6](#), [7](#)
- [88] Kai Zhang, Wangmeng Zuo, and Lei Zhang. Learning a single convolutional super-resolution network for multiple degradations. In *Proceedings of the IEEE Conference on Computer Vision and Pattern Recognition*, pages 3262–3271, 2018. [5](#), [6](#)
- [89] Zhao Zhong, Junjie Yan, Wei Wu, Jing Shao, and Cheng-Lin Liu. Practical block-wise neural network architecture generation. In *Proceedings of the IEEE conference on computer vision and pattern recognition*, pages 2423–2432, 2018. [3](#)
- [90] Fengyuan Zhu, Guangyong Chen, and Pheng-Ann Heng. From noise modeling to blind image denoising. In *Proceedings of the IEEE Conference on Computer Vision and Pattern Recognition*, pages 420–429, 2016. [2](#)
- [91] Barret Zoph and Quoc V Le. Neural architecture search with reinforcement learning. *arXiv preprint arXiv:1611.01578*, 2016. [3](#)
- [92] Barret Zoph, Vijay Vasudevan, Jonathon Shlens, and Quoc V Le. Learning transferable architectures for scalable image recognition. In *Proceedings of the IEEE conference on computer vision and pattern recognition*, pages 8697–8710, 2018. [3](#)
- [93] Daniel Zoran and Yair Weiss. From learning models of natural image patches to whole image restoration. In *2011 International Conference on Computer Vision*, pages 479–486. IEEE, 2011. [2](#), [6](#), [7](#)